

SYNTHESIS AND STRUCTURAL ANALYSIS OF COBALT OXIDE NANOPARTICLES

Dr.V.Revathi¹,Dr.R.Purushothaman²,Dr.K.Ezhumalai³,Ms.R.Jayasri⁴.

Assistant Professor Department of Physics DhanalakshmiSrinivasan College of Arts &
Science for Women

Abstract

Cobalt (II, III) oxide is an inorganic compound with the formula Co_3O_4 . It is a black antiferromagnetic solid. As a mixed valence compound, its formula is sometimes written as $\text{Co}^{\text{II}}\text{Co}_2^{\text{III}}\text{O}_4$ and sometimes as $\text{CoO}.\text{Co}_2\text{O}_3$. The XRD result confirmed the formation of simple cubic crystal structure of the Co_3O_4 . The average crystallite size of the samples are found to increase with increase in annealing temperature. The optical energy band gap values estimated by UV-visible analysis reported that the energy band gap values are increased with increase in calcination temperature. So that Co_3O_4 nanoparticles are used as p-type semiconductor. The Photoluminescence sharp peaks shows a near and edge emission located at UV region and green emissions.

Key Words: Cobalt oxide nanoparticles, XRD, UV Analysis.

1.1 Introduction

Nanotechnology can be defined as research and technology development at the atomic, molecular or macro molecular levels in the length scale of approximately 1-100 nanometers [1]. The idea of nanotechnology was first recognized by noble prize winner, an American scientist Richard Feynman who said "There is plenty of room at bottom". There are endless possibilities for improved devices, structures and materials if we can understand these differences and learn how to control the assembly of small structures. Nanotechnology, which is one of the novel technologies, discusses to the development of structures, devices and systems having size 1-100 nm [2]. Currently, nanotechnology is expected to be powerful technology in next 20-30 years in all fields of science and technology. It has capacity to control, appreciate and operate matter at the level of individual atoms and molecules [3].

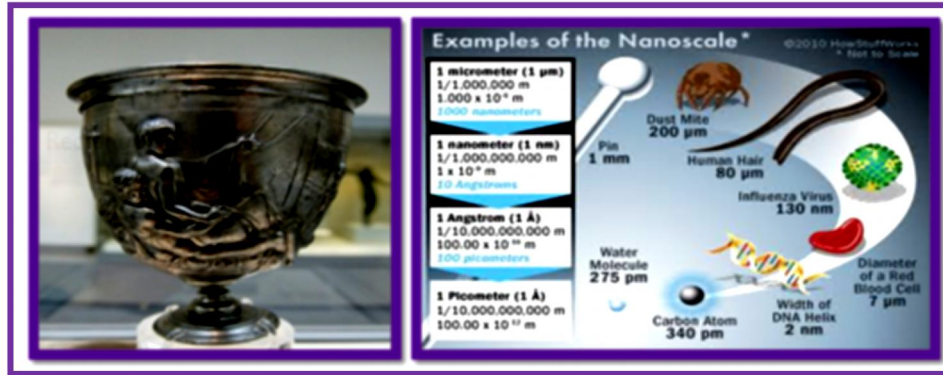


Fig. 1.1: Examples of nanotechnology and nanoscale materials

There are many examples of nanostructures in nature in the way that plants and animals. Natural nanoscale materials such as catalysts, porous, certain minerals, soot particles. Before thousands of years, several nanomaterials were used for medical and esthetical purpose like colloidal gold metals was used to develop ruby glass and also colored ceramics. Fig. 1.1 shows the examples of nanotechnology and nanoscale materials.

Nanotechnology used to reduce the cost of catalysts used in fuel cells. It can be used in sensors to detect elements such as carbon nanotubes, zinc oxide nanowire based on the sensor. It is used in medicine to reduce damage to healthy cells in the body and allows for earlier detection of disease. Ex: chemotherapy [1].

1.2. Classification of nanomaterials

Nanomaterials which are belonging to resource of nature defined as “natural nanomaterials”. As per example virus, protein molecules including antibody originated from nature. In addition minerals such as clays, natural colloidal, such as milk and blood (liquid Colloids), fog (aerosol type), gelatin (gel type), mineralized natural materials such as shells, corals and bones, insect wings and opals, spidersilk etc. Fig. 1.2 shows the natural nanomaterials

on earth. Artificial nanoparticles are those which are prepared through a well defined mechanical and fabrication process. The examples of such materials are carbon nanotubes, semiconductor nanoparticles like quantum dots etc.

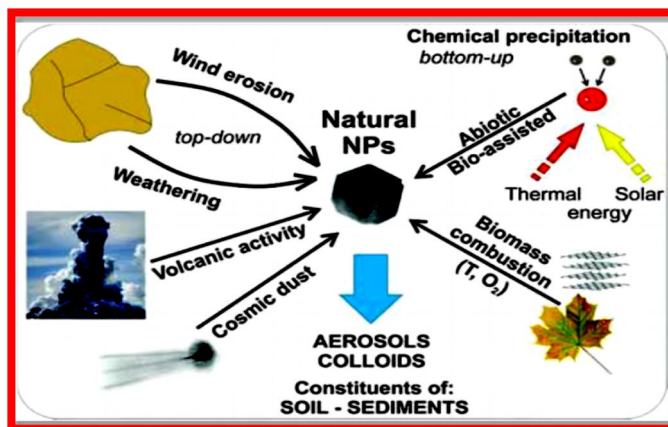


Fig. 1.2: Natural nanomaterials on earth

1.1.1. According to the dimensions

Zero dimensional: These nanomaterials have nano dimensions in all the three directions. Metallic nano particles including gold and semiconductor such as quantum dots are the perfect examples. Most of these nanoparticles are spherical in size and the diameter of these particles will be in the 1 – 50 nm range.

One dimensional: These nanostructures of one dimension will be outside the nanometer range. These include nano wires, nano rods and nano tubes. These materials are long (micrometer in length), but with diameter of only a few nanometer. Nanowire and nanotubes of metals, oxides are few examples. Fig. 1.3 shows the classification of nanomaterials under dimensions.

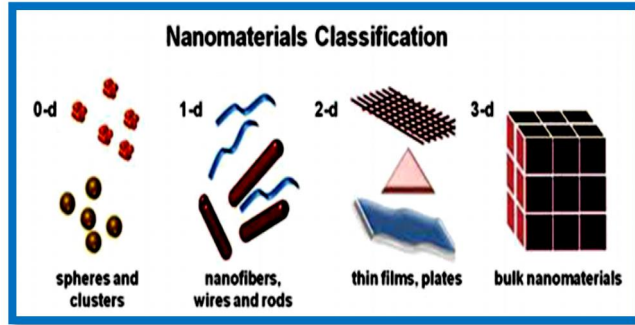


Fig. 1.3: Classification of nanomaterials under dimensions

Two dimensional: This type of nanomaterials also outside the nanometer range. These include different kind of nanofilms such as coatings and thinfilm – multilayer nano sheets or nanowalls. The area of the nanofilms can be large, but the thickness is always in nano scale range.

Three dimensional: All dimensions of these are outside the nanometer range. These include bulk materials composed of the individual blocks which are in the nanometer scale.

1.2.1. On the basis of structural configuration

Carbon based nanomaterials: The nature of this kind of nanomaterials is hollow spheres, ellipsoids or tubes. Spherical and ellipsoidal configured carbon nanomaterials are defined as fullerenes, while cylindrical ones are described as nanotubes. Fig. 1.4 shows the classification of nanomaterial under structural configuration.

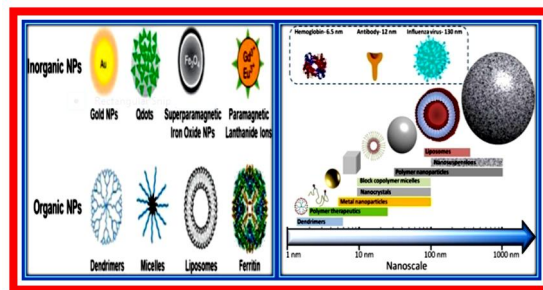


Fig. 1.4: Classification of nanomaterial under structural configuration

Metal based materials: The main component of these particles is metal. These nanomaterials include nanogold, nanosilver and metal oxides, such as titanium dioxide and closely packed semiconductor like quantum dots.

Dendrimers: Dendrimers are highly branched macromolecules with the dimensions in nanometer scale. The surfaces of a dendrimer possess numerous chains which can be modified to perform specific chemical functions. PAMAM dendrimers is the best illustration of this kind of materials.

Composites: Nano composite can be described as a multiphase solid material where at least one of the phases has one, two or three dimensions in nanoscale. The most common examples of these materials are colloid and gels [4].

1.3. Properties of nanomaterials

1.3.1. Physical properties

- Large fraction of surface atoms.
- Large surface energy.
- Spatial confinement.
- Reduced imperfections.
- Nanomaterials may have a significantly lower melting point or phase transition temperature and appreciably reduced lattice constants due to a huge fraction of surface atoms in the total amount of atoms.
- Mechanical properties of nanomaterials may reach the theoretical strength, which are one or two orders of magnitude higher than that of single crystals in the bulk form. The enhancement in mechanical strength is simply due to reduced probability of defects.

- Optical properties of nanomaterials can be significantly different from bulk crystals. For example, the optical absorption peak of a semi conductor nanoparticle shifts to a short wavelength, due to an increased band gap. The color of metallic nanoparticles may change with their sizes due to surface plasmon resonance. Fig. 1.5 shows the changes in the property of nanomaterials from the bulk materials.

1.3.2. Chemical properties

- Chemical properties of nanomaterials also change at nano scale. As the percentage of surface atoms in nano particles is large compared with bulk objects, therefore reactivities of nanomaterials are more than bulk materials.
- The preponderance of surface is a major reason for the change in behavior of materials at the nanoscale. As up to half of all the atoms, properties such as electrical transport are no longer determined by solid state bulk phenomenon.
- The atoms in nanomaterials have a higher average energy than atoms in longer structures, because of the large proportion of surface atoms. For example, catalytic materials have a greater chemical activity per atom of exposed surface as the catalyst is reduced in size at the nanoscale.
- Defects and impurities may be attracted to surface and interfaces and interactions between particles of those small dimensions can depend on the structure and nature of chemical bonding at the surface.
- Molecular monolayer may be used to change or control surface properties and to mediate the interaction between nanoparticles.

1.3.3. Magnetic properties

- Magnetic nanoparticles are used in a range of applications like imaging, bioprocessing, refrigeration as well as high storage density magnetic memory media.
- The large surface area to volume ratio results in a substantial proportion of atoms having different magnetic coupling with neighboring atoms leading to differing magnetic properties.
- Bulk gold and platinum are non magnetic but at the nano size they act as magnetic particles. Au nanoparticles become ferromagnetic when they are capped with the appropriate molecular such as thiol.
- Giant magneto resistance (GMR) is a phenomenon observed in nanoscale multilayer consisting of strong ferromagnet (Fe, Co, Ni) and a weaker magnetic or non-magnetic buffer (Cr, Cu). It is usually employed in data storage and sensing.

1.3.4. Optical property

- In small nano clusters the effect of reduced dimensionality on electronic structure has the most profound effect on the energies of highest occupied molecular orbital (HOMO) which is valance band the lowest unoccupied molecular orbital (LUMO), essentially the conduction band.
- The optical emission and adsorption occurs between these two states.
- Semiconductor and many metals show large change in optical properties such as color, as a function of particle size.
- Colloidal suspense of gold nanoparticles have a deep red color which becomes progressively more yellow as the particle size increases.

- Gold spheres of 10-20nm exhibit red color.
 - Silver particles of 40nm exhibit blue color.
 - Prism shaped silver particles are red color.
- Other properties which may be affected by reduced dimensionality include photo catalysis, photo conductivity, photoemission and electroluminescence [4].

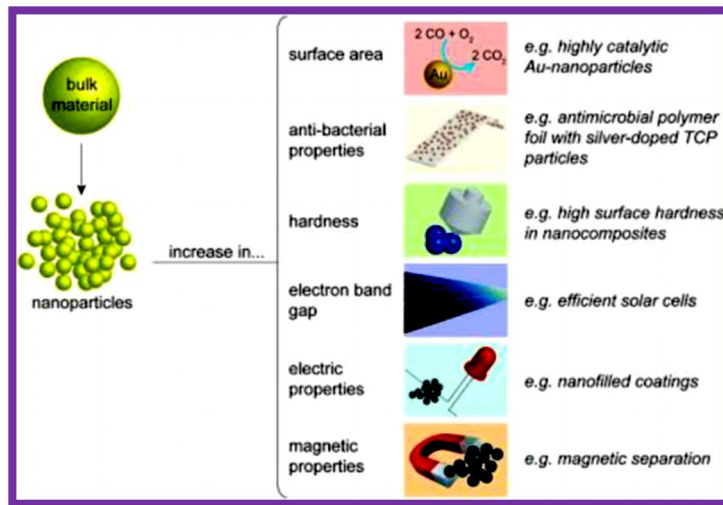


Fig. 1.5: Properties of nanomaterials

1.4. Applications of nanomaterials

- **Cosmetics application of nanoparticle:** E.g. sunscreen lotions: (reabsorb properties).
- **Nanocomposites:** Nanoparticle silicate nanolayer (clay nanocomposites) and nano tubes can be used as reinforced filler not only to increase mechanical properties of nanocomposites but also to import new properties (optical, electronic etc).
- **Nanocoatings:** Surface coating with nanometer thickness of nanomaterial can be used to improve properties like wear and scratch-resistant, optoelectronics, hydrophobic properties.

- **Hard cutting tools:** Current cutting tools (e.g. mill machine tools) are made using a sort of metal nano composites such as tungsten carbide, tantalum carbide and titanium carbide that have more wear and erosion-resistant, and last longer their conventional (large-grained) materials.
- **Fuel cells:** Could use nano-engineered membranes for catalytic processes to improve efficiency of small-scale fuel cells.
- **Display:** New class of display using carbon nanotubes as emission device for the next generation of monitor and television (FED- field emission displays).
- **Drug delivery systems:** One of the most potential applications of nanotechnology might be related to gene and drug delivery system in order to improve therapy efficacy. The challenge is devise nanoparticle capable of targeting specific disease cells, which contains both therapeutic agents that are released into the cell and on board sensor that regulates the release.
- **Medical imaging for diagnosis:** Nanotechnologies already use quantum dots or synthetic chromophores to select molecules (e.g. proteins) for intracellular imaging. Also incorporation of naturally fluorescent proteins has been experimented which with optical techniques allow intracellular biochemical processes to be investigated directly [1].

1.5. Material introduction

1.5.1. Transition metal oxide

Transition metal oxides constitute probably one of the most interesting classes of solids, exhibiting a variety of structures and properties. The nature of metal oxygen bonding can vary between nearly ionic to highly covalent or metallic. The unusual properties of transition metal oxides are clearly due to the unique nature of the outer d-electrons. These materials can have

useful electronic and magnetic properties. Many of these properties strongly depend on materials defects like vacancies, dislocations, stacking faults and grain boundaries. These defects affect local oxygen bonding. Transition metal oxides are used in a wide variety of technologically important catalytic processes. For example, they are used in selective oxidation, selective reduction and dehydrogenation. Understanding surface structure and reactions is important for understanding these catalytic processes. In periodic table, Groups 3-12 are called the transition elements and all of them are metal. Most of the transition elements are found combined with other elements in ores. A few transition elements such as gold and silver are found as pure elements. There are two series of inner transition elements. The first series, from cerium to lutetium, is called the lanthanides. The second series of elements from thorium to lawrencium is called actinides. Other transition elements such as iron, cobalt and nickel have magnetic properties. Nickel, zinc and cobalt can be used as catalyst. As catalysts, the transition elements are used to produce electronic and consumer goods, plastic and medicines [5]. In different fields of science and technology cobalt based oxide materials have captured a lot of interest among the research community because of their potential applications due to its nanostructure forms. Hence, in the present work, we aim to prepare Co_3O_4 nanoparticles.

1.5.2. Cobalt (II, III) oxide

Cobalt (II, III) oxide is an inorganic compound with the formula Co_3O_4 . It is a black antiferromagnetic solid. As a mixed valence compound, its formula is sometimes written as $\text{Co}^{\text{II}}\text{Co}_2^{\text{III}}\text{O}_4$ and sometimes as $\text{CoO}.\text{Co}_2\text{O}_3$. Cobalt has two stable oxide states known as CoO and Co_3O_4 . At room temperature both compounds are found to be kinetically stable. Co_3O_4 is an important magnetic p-type semiconductor having direct optical band gaps as 1.48 and 2.19 eV. Table 1.1 shows the physical properties of Co_3O_4 . The conductivity is usually p-type at low

temperature and intrinsic at high temperature. Co_3O_4 adopts the normal spinel structure, with Co^{2+} ions in tetrahedral interstices and Co^{3+} ions in the octahedral interstices of the cubic close packed lattice arrays of oxide anions as shown in Fig. 1.7. Cobalt (II, III) oxide structure and cobalt (II) oxide structure are shown in the Fig. 1.6. As a result, the Co^{3+} ions are not magnetic, whereas the Co^{2+} ions carry a magnetic moment. Co_3O_4 is a paramagnetic semiconductor at room temperature. It becomes antiferromagnetic below $T_N \sim 40\text{K}$, where the antiferromagnetism is mainly due to the weak coupling between nearest neighbour Co^{2+} ions.

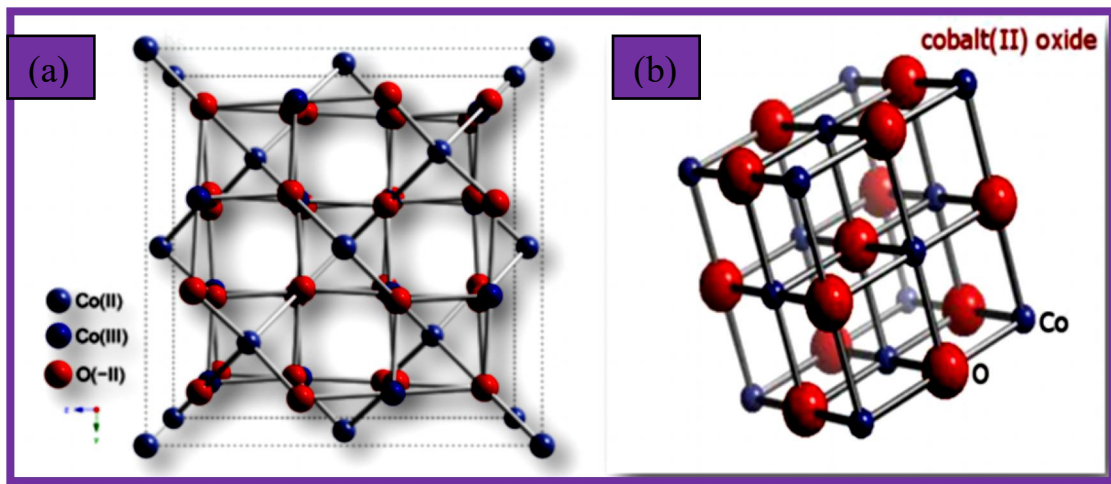


Fig. 1.6: (a) Cobalt (II, III) oxide structure, (b) Cobalt (II) oxide structure

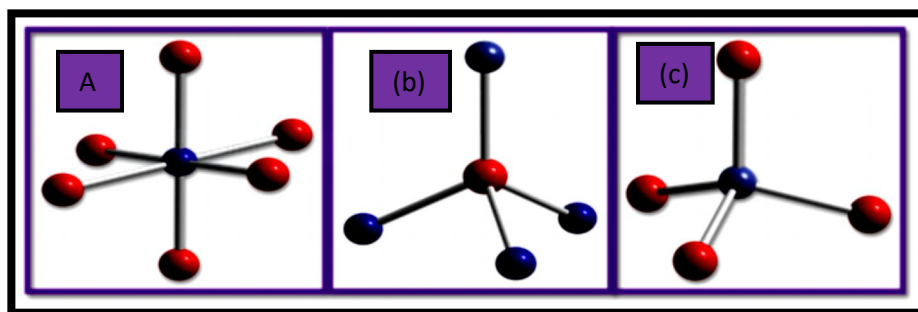


Fig. 1.7: a) Tetrahedral co-ordination geometry of Co(II) , b) Distorted octahedral co-ordination geometry of Co(III) and c) Distorted tetrahedral co-ordination geometry of O

Till now various methods have been used to prepare high quality of Co_3O_4 nanoparticles. However, chemical techniques like sol-gel method, co-precipitation method, hydrothermal method, sonochemical synthesis and micromulsion route are particularly attractive for large surface area to volume ratio. Among these methods, sol-gel technique has advantages like low temperature process, smaller particle size and morphological control, better homogeneity and phase purity comparable to the other methods. This method is widely used in the synthesis of inorganic and organic-inorganic hybrid materials and capable of producing nanoparticles, nano rods and thin films. Therefore, we have used sol-gel technique to prepare Co_3O_4 nanoparticle.

Table1.1: Physical properties of Co_3O_4

Chemical formula	Co_3O_4
Molar mass	240.80g /mol
Appearance	Block solid
Density	6.11g /cm ³
Melting point	895°C (1643°F, 1168K)
Boiling point	900°C (1650°F, 1170K)
Solubility in water	Insoluble
Solubility	Soluble in acids and alkalis
Refractive index	1.4 – 8.2

Magnetic susceptibility	$+7380.10^{-6}\text{cm}^3/\text{mol}$
Crystal structure	Cubic

1.7. Scope of the work

The aim of this present work is to present cobalt oxide (Co_3O_4) nanoparticles by sol gel method and to study their properties by the influence of various annealing temperatures.

The objectives of the study are:

- To prepare Co_3O_4 nanoparticles by sol gel method.
- To study the annealing temperature induced change in its properties.
- Study the structural, morphological properties of Co_3O_4 nanoparticles by X-ray diffraction Study the optical properties of the samples by UV-visible spectroscopy and Photoluminescence.

CHAPTER – II

SYNTHESIS METHODS AND CHARACTERIZATION TECHNIQUES

2.1. Introduction

Nanocrystalline materials can be synthesized either by consolidating atoms/molecules/clusters or breaking down the bulk material into smaller and smaller dimensions. The former is known as the “Bottom up” approach, whereas, the latter is referred to as the “Top down” method. Many techniques including both Top-down and Bottom up approaches have been developed and applied for the synthesis of nanoparticles. In the Top-down approach a block of a bulk material is whittled or sculptured to get the nanosized particle. The Top-down approaches include milling or attrition, lithography etc. The main disadvantage of Top-down approach is the imperfection of the surface structure. The nanoparticles produced by the attrition have a relatively broad size distribution and various particle shape or geometry. In addition they may contain significant amount of impurities. In the Bottom-up approach, the individual atoms and molecules are placed or self assembled precisely where they are needed. Here the molecules or atomic building blocks fit together to produce nanoparticles. Bottom-up approaches are more favorable and popular in the synthesis of nanoparticles and many preparation techniques of Bottom-up approach have been developed. Fig. 2.1 shows two approaches of synthesis of nanoparticles. Some of the chemical methods for the synthesis of nanoparticles are discussed in following sections.

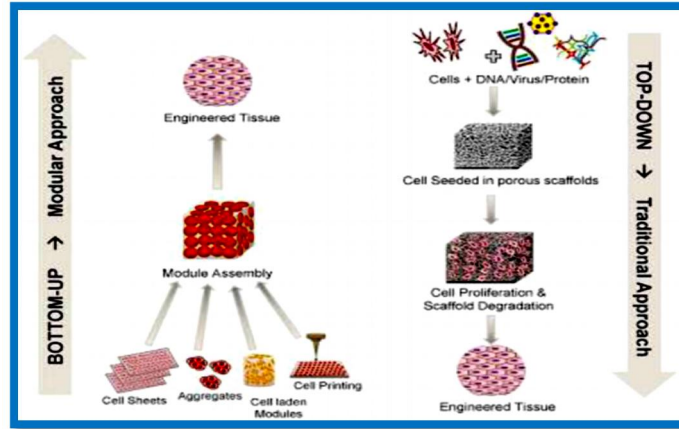


Fig. 2.1: Two approaches of synthesis of nanoparticles

2.2. Co-precipitation method

In this process, the required metal cations from a common medium are co-precipitated usually as hydroxides, carbonates, oxalates, formates or citrates. These precipitates are subsequently calcinated at appropriate temperatures to yield the final powder. For achieving high homogeneity, the solubility products of the precipitate of metal cations must be closer. Co-precipitation results in atomic scale mixing and hence, the calcining temperature required for the formation of final product is low, which lead to lower particle size. However, each synthesis requires its own special conditions, precursor reactions, etc. Also co-precipitation process required to control the concentration of the solution, pH, temperature and stirring speed of the mixture in order to obtain the final product with required properties.

Advantages of co-precipitation method

- Homogeneous mixing of reactant precipitates reduces the reaction temperature.
- Simple direct process for the synthesis of fine metal oxide powders, which are highly reactive in low temperature sintering.

Disadvantages of co-precipitation method

- This process is not suitable for the preparation of high pure, accurate stoichiometric phase.
- This method does not work well, if the reactants have very different solubility as well as different precipitation rate.
- It is not having universal experiment condition for the synthesis of various types of metal oxides.

2.3. Sol-Gel method

Sol-gel is the multi step process, involving chemical and physical processes associated with hydrolysis, polymerization, gelation, condensation, drying and densification. This process generally starts with the mixing of metal alkoxides or salts in water or in a suitable solvent (usually alcohol) at ambient or slightly elevated temperature. In sol-gel process, controlling the pH of the starting solution is very much important to avoid the precipitation as well as to form the homogenous gel, which can achieve by the addition of base or acidic solution. Apart from the above, organic compounds with hydrophilic functional groups (hydroxides or carboxylates) in small molecules such as citric acid, succinic acid, oxalic acid, tartaric acid, acrylic acid, etc and polymers like polyacrylic acid (PAA) and polyvinyl pyrrolidone (PVP) can be used with metal ion sources to form the sol as well as control the particle size and uniformity of the products. Chelation of metal ions by carboxylic acid groups lead to a homogeneous distribution of the constituent ions in the obtained gel. The gel intermediate is further heated between 150 °C and 300 °C to eliminate volatile organic components, excess water, etc., which results the dried intermediate powders. Single phase nanocrystalline metal oxides are obtained after calcining of

dried gel powder at 400°-800°C depends on the precursor chemical nature. Fig. 2.2 shows the steps involved in sol gel method to produce final product.

Advantages of sol gel method

- Low temperature processing and consolidation is possible.
- Smaller particle size and morphological control in powder synthesis.
- Sintering at low temperature is also possible.
- Better homogeneity and phase purity compared to traditional ceramic method.

Disadvantages of sol gel method

- Raw materials for this process is expensive (in the case of metal alkoxides) compared to mineral based metal ion sources.
- Products would contain high carbon content when organic reagents are used in preparative steps and this would inhibit densification during sintering.
- Since several steps are involved, close monitoring of the process is needed [16].

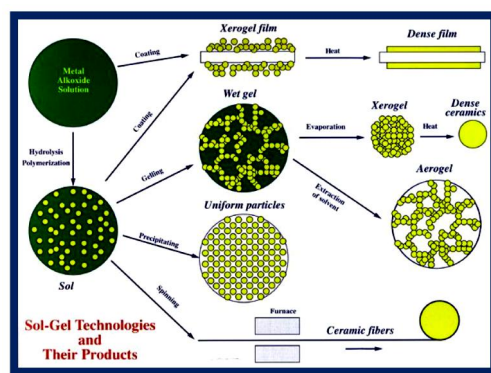


Fig. 2.2: Steps involved in sol-gel method

2.4. Characterization techniques

2.4.1. Powder X-ray diffraction (XRD)

X-ray diffraction technique is the most common and efficient method for the determination of structure, crystallinity and material identification. XRD examines whether a resultant material has amorphous or crystalline nature. Crystalline phases can be identified by just comparing the interplanar distance 'd' values obtained from XRD data with the fundamental data in Joint Committee on Powder Diffraction Standards (JCPDS). X-ray diffraction is based on constructive interference of monochromatic X-rays from a crystalline sample. The X-rays, generated by a cathode ray tube are filtered to produce monochromatic radiation, collimated and directed towards the sample. X-rays primarily interact with electrons in atoms, collide and some photons from the incident beam are deflected away from original. The X-rays interfere constructively and destructively producing a diffraction pattern on the detector. The incident X-ray radiation produces a Bragg peak if their reflections from the various planes interfered constructively. The interference is constructive, when the phase shift is a multiple of 2π , this condition can be expressed by Bragg's law ($n\lambda = 2d \sin\theta$) where, n is an integer, λ is the wavelength of incident wave, d is the spacing between the planes in the atomic lattice and θ is the angle between the incident ray and the scattering planes. Fig. 2.3 shows the principle of X-ray diffraction.

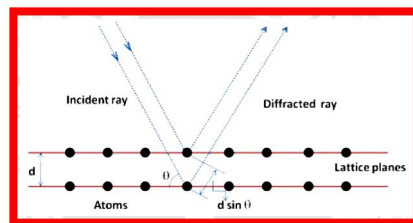


Fig. 2.3: Principle of X-ray diffraction

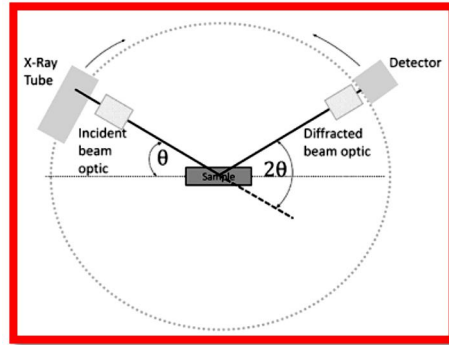


Fig. 2.4: Schematic diagram of X-ray diffractometer

A typical powder X-ray diffractometer consists of a source of radiation, a monochromator to choose the wavelength, slits to adjust the shape of the beam, a sample and a detector. A goniometer is used for fine adjustment of the sample and the detector positions. The goniometer mechanism supports the sample and detector, allowing precise movement. The source of X-rays contains several components; the most common being K_{α} and K_{β} . The specific wavelengths are the characteristic of the target material (Cu, Fe, Mo and Cr). Monochromators and filters are used to absorb the unwanted emission with wavelength K_{β} , while allowing the desired wavelength, K_{α} to pass through. The X-ray radiation most commonly used is that emitted by copper, whose characteristic wavelength for the K_{α} radiation is equal to 1.54 Å. The filtered X-rays are collimated and directed onto the sample. When the incident beam strikes a powder sample, diffraction occurs in every possible orientation of 2θ . The diffracted beam may be detected by using a moveable detector such as a Geiger counter, which is connected to a chart recorder. The counter is set to scan over a range of 2θ values at a constant angular velocity. Routinely, a 2θ range of 5 to 70 degrees is sufficient to cover the most useful part of the powder

pattern. The scanning speed of the counter is usually 2θ of 2° min^{-1} . A detector records and processes this X-ray signal and converts the signal to a count rate which is then fed to a device such as a printer or computer monitor. Fig. 2.4 shows the schematic diagram of X-ray diffractometer. The sample must be ground to fine powder before loading it in the glass sample holder. Sample should completely occupy the square glass well. The structural property of prepared Co_3O_4 nanoparticle was studied by X-ray diffraction.

2.4.2. UV-Visible Spectroscopy

UV spectroscopy is a type of absorption spectroscopy in which light of ultra-violet region (200-400 nm) is absorbed by the molecule. Absorption of the ultra-violet radiations results in the excitation of the electrons from the ground state to higher energy state. UV spectroscopy obeys the Beer-Lambert law, which states that when a beam of monochromatic light is passed through a solution of an absorbing substance, the rate of decrease of intensity of radiation with thickness of the absorbing solution is proportional to the incident radiation as well as the concentration of the solution. The expression of Beer-Lambert law is

$$A = \log (I_0/I) = \epsilon cl$$

where,

- A= absorbance.
- I_0 = intensity of light incident upon sample cell.
- I = intensity of light leaving sample cell.
- l = length of sample cell.
- ϵ = molar attenuation coefficient.

From the Beer-Lambert law, it is clear that greater the number of molecules capable of absorbing light of a given wavelength, the greater the extent of light absorption. The basic principle of UV spectrophotometer is shown in the Fig. 2.5.

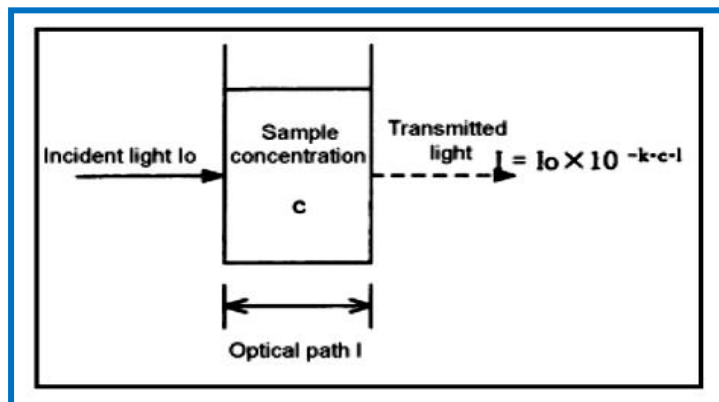


Fig. 2.5: Principle of UV-Vis Spectrophotometer

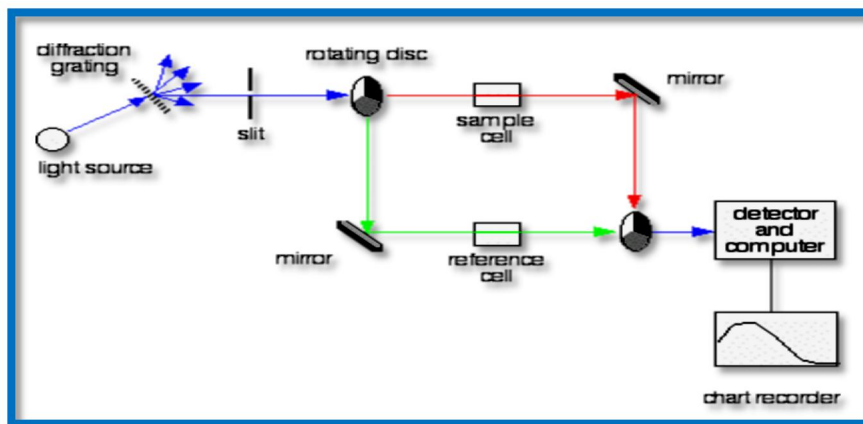


Fig. 2.6: Schematic diagram of UV-Vis spectrophotometer

The main components of the UV-Vis spectrophotometer are a light source, double beams (reference and sample beam), a monochromator, a detector and a recording device. The source is usually a tungsten filament lamp for visible and deuterium discharge lamp for UV measurements. The light coming out of the source is split into two beams - the reference and the

sample beams as shown in the Fig. 2.6. The sample and reference cells are rectangular quartz / glass containers; they contain the solution (to be tested) and pure solvent, respectively. The spectrophotometer records the ratio between the reference and sample beam intensities. The recorder plots the absorbance (A) against the wavelength (λ). The sample is prepared into a paste and then dissolved into the solvent to make a dilute sample solution. This sample solution is filled up to mark line of the sample cell. The optical properties of samples were studied by UV-Vis spectrophotometer.

2.4.3. Photoluminescence (PL) Spectroscopy

Photoluminescence spectroscopy is a contactless, nondestructive method of probing the electronic structure of materials. Light is directed onto a sample, where it is absorbed and imparts excess energy into the material in a process called photo excitation. Photo excitation causes electrons within a material to move into permissible excited states. When these electrons return to their equilibrium states, the excess energy is released and may include the emission of light (a radiative process) or may not (a nonradiative process). Other way this excess energy can be dissipated by the sample through the emission of light or luminescence. In the case of photo excitation, this luminescence is called photoluminescence. Photoluminescence implies both Fluorescence and Phosphorescence.

- Fluorescence – ground state to singlet state and back.
- Phosphorescence – ground state to triplet state and back.

A typical PL experiment in semiconductor can be divided into three stages: Firstly, the sample is excited from ground state, which is a completely filled valence band (VB) to the empty conduction band (CB), energy pumped for excitation is $\hbar\omega$ pump. The laser creates electron-hole

pairs due to a transfer of electrons from VB into CB. Secondly, the non-equilibrium electron and hole distributions tend to relax into the ground state. The initial intraband relaxation is caused by energy transfer to the crystal lattice, i.e. a step by step excitation of lattice vibration. Finally, the electron-hole pair recombines accompanied by the emission of light which is a photoluminescence process. Fig. 2.7 shows the principle of photo luminescence spectroscopy.

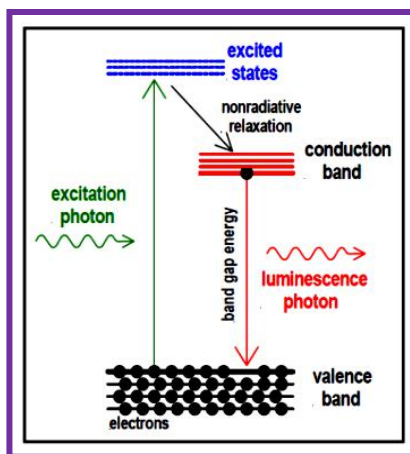


Fig. 2.7: Principle of Photoluminescence spectroscopy

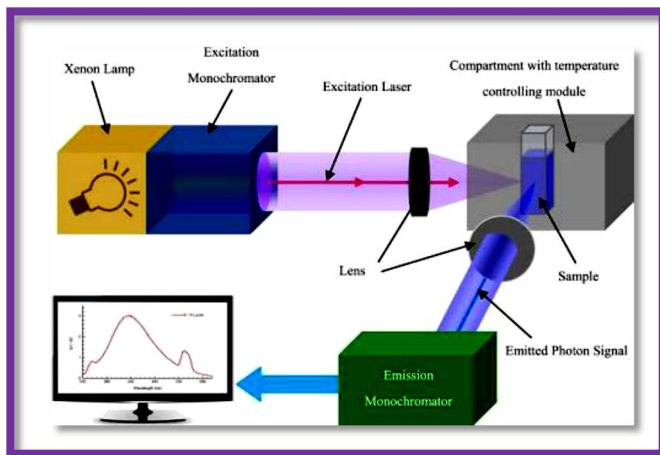


Fig. 2.8: Schematic diagram of a fluorescence spectrometer

The fluorescence instruments contain three basic items: a source of light, a sample holder and detector. The light source produces light photons over a broad energy spectrum, typically ranging from 200 to 900 nm. Photons impinge on the excitation monochromator, which selectively transmits light in a narrow range centered about the specified excitation wavelength. The transmitted light passes through adjustable slits that control magnitude and resolution by further limiting the range of transmitted light. The filtered light passes into the sample cell causing fluorescent emission by fluorophors within the sample. Emitted light enters the emission monochromator, which is positioned at a 90° angle from the excitation light path to eliminate background signal and minimize noise due to stray light. Again, emitted light is transmitted in a narrow range centered about the specified emission wavelength and exits through adjustable slits, finally entering the photomultiplier tube (PMT). The signal is amplified and creates a voltage that is proportional to the measured emitted intensity. Noise in the counting process arises primarily in the PMT. Therefore, spectral resolution and signal to noise is directly related to the selected slit widths. Fig. 2.8 shows the schematic diagram of a fluorescence spectrometer. Sample preparation process is same as that of UV - Visible spectroscopy. In both the cases, the sample cell (cuvette) must be free from contaminants. The photoluminescence property of the synthesized sample was studied using PL spectroscopy.

CHAPTER – III

PREPARATION OF Co_3O_4 NANOPARTICLES BY SOL-GEL METHOD AND THEIR RESULTS

3.1. Introduction

Nanostructured materials have been widely investigated for the fundamental scientific and technological interests in accessing new classes of fundamental materials with unprecedented properties and applications. Inorganic nanomaterials have more attention because of the vast application as electrical, optical and magnetic properties [9]. In nanosized co-particles display a wide range of interesting size-dependent catalytic properties. In particular, because of their large surface area, co-nanoparticles showed high chemical reactivity which makes them suitable for catalysis. Co_3O_4 nanopowder which is p-type semiconductor and widely used in many fields such as magnetic, gas sensor, catalysis and electrochemical based on size, structure, shape, phase and surface morphology. Cobalt oxide plays an efficient role in memory storage [7]. In the present investigation, we have attempted to synthesize Co_3O_4 nanoparticles by sol-gel method at low temperature and study its optical, structural and morphological properties.

3.2. Preparation of Co_3O_4 nanoparticles

Cobalt acetate is a moderately water soluble crystalline cobalt source that decomposes to cobalt oxide on heating. It is generally immediately available in most volumes. All metallic acetates are inorganic salts containing a metal cation and the acetate anion. Acetates are excellent precursors for the production of ultra high purity compounds, catalysts and nanoscale material.

Oxalic acid is an organic compound with the formula $C_2H_2O_4$. It is a colorless crystalline solid that forms a colorless solution in DI water. It is used as an analytical reagent and general reducing agent.

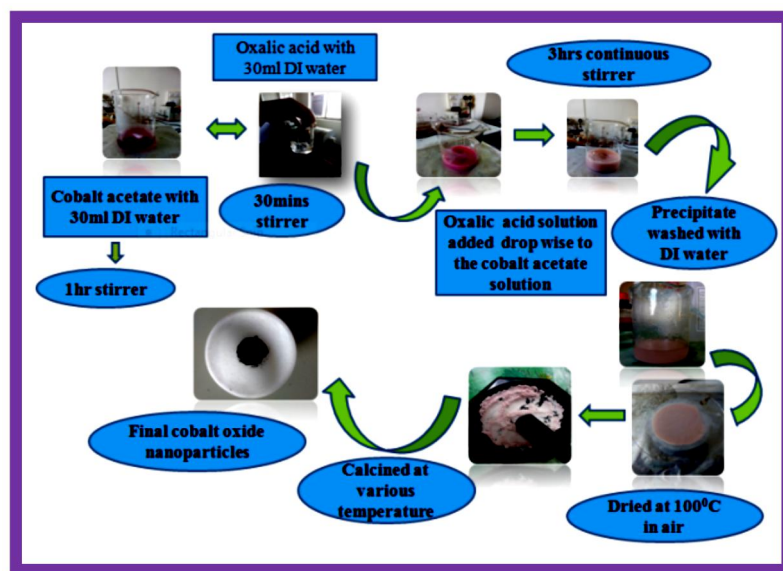


Fig. 3.1: Schematic representation of preparation method

The schematic representation of synthesis process is shown in Fig. 3.1. Cobalt acetate (0.3 M) solution was prepared by double distilled water (30 ml) and continuous stirring for 1 hr. Aqueous oxalic acid (0.3 M) solution was drop wise added to the cobalt acetate solution with continuous stirring for three hours. The resultant light pink coloured precipitates thus obtained were washed with double distilled water and then dried at 100°C for 4 hrs. The synthesized powder was calcinated at various temperatures such as 200°C, 300°C, and 400°C. Finally, black color Co_3O_4 nanoparticles were obtained.

3.3. Results and discussion

The results of various characterization studies on Co_3O_4 nanoparticles are discussed in the following sections.

3.3.1. Structural study

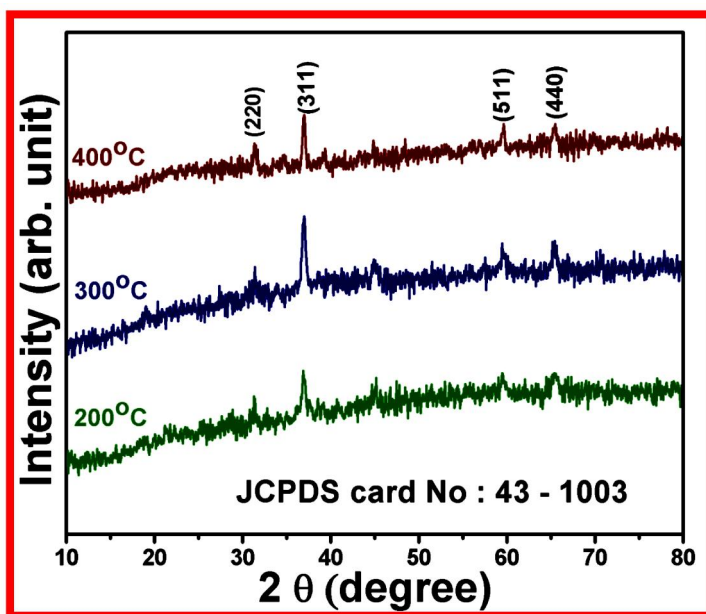


Fig. 3.2: XRD patterns of Co_3O_4 nanoparticles with different annealing temperatures

The phase and crystalline nature of the Co_3O_4 nanoparticles calcinated at 200° C, 300° C and 400° C were characterized by X-ray diffraction. The XRD patterns of Co_3O_4 nanoparticles annealed at different temperatures are shown in Fig. 3.2. The diffraction peaks observed at the 2θ values of 31.3°, 36.9°, 59.5°, 65.5° are comparable with the standard JCPDS data card No: 43-1003, which revealed the formation of cubic phase Co_3O_4 . The diffraction pattern indicates the

purity of the sample as there were no other peaks present which indicate the absence of the other phases like CoO, Co₂O₃.

The average crystallite size of Co₃O₄ nanoparticles were estimated using Debye-Scherrer's formula

$$D = \frac{k\lambda}{\beta \cos\theta}$$

where,

- D – Crystallite size
- K – Dimensionless shape factor
- λ- Wavelength of X-ray source
- β- Full width half maximum
- θ- Bragg's angle

The dislocation density (δ) of the samples was calculated using the relation:

$$\delta = \frac{1}{D^2}$$

Micro-strain (ε) also calculated using the formula:

$$\varepsilon = \frac{\beta \cos\theta}{4}$$

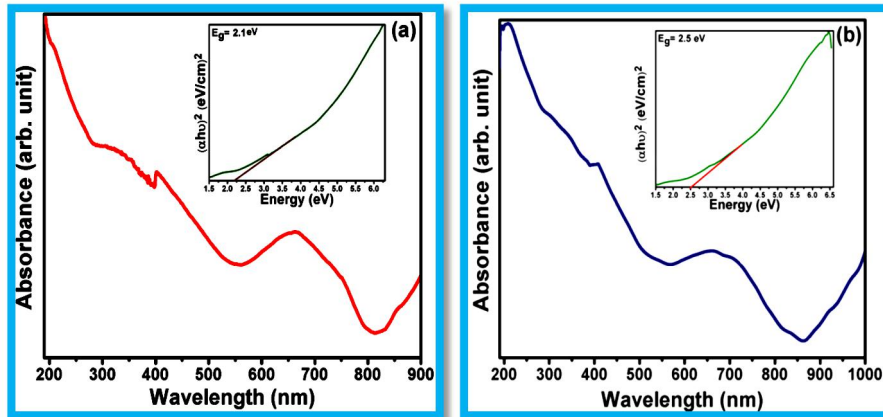
The calculated structural parameters are summarized in Table 3.1. The average crystalline size of the Co₃O₄ nanoparticles calcinated at 200° C, 300° C and 400° C were calculated to be 15 nm, 16 nm, 27 nm respectively [8]. The lattice parameter of synthesized sample was determined according to the following relation and its value is a=1.645 Å

$$\frac{1}{d^2} = \frac{h^2 + l^2 + k^2}{a^2}$$

Table 3.2: Structural parameters analysis of Co₃O₄ nanoparticles

Sample	Annealing Temperature	Crystalline size (D) in nm	Dislocation density (δ) ×10 ⁻³ lines/m ²	Strain (ε) × 10 ⁻³ Lines ⁻² /m ⁻⁴
Co ₃ O ₄ (0.3M)	200°C	15	6.813	2.646
	300°C	16	1.789	1.407
	400°C	27	6.863	3.881

3.3.2. UV-Visible spectrophotometer result



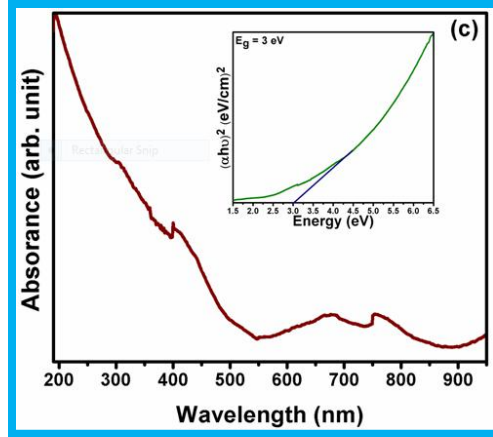


Fig. 3.3: Optical absorbance spectra of calcinated Co_3O_4 nanoparticles at (a) 200°C , (b) 300°C and (c) 400°C . Insets show the Tauc plots.

The optical absorption spectra of the Co_3O_4 nanoparticles were carried out using UV-vis spectrophotometer. Fig. 3.3 shows the absorption spectra of synthesized nanoparticles at various calcinated temperatures. The optical absorption shows two peaks in the visible region, which can be assigned to the $\text{O}^{2-} \rightarrow \text{Co}^{2+}$ and $\text{O}^{2-} \rightarrow \text{Co}^{3+}$ charge transfer processes [12].

The optical energy band gap of Co_3O_4 nanoparticles were estimated from absorption coefficient (α) and photon energy ($h\nu$) using the Tauc's relation

$$(\alpha h\nu) = A(h\nu - E)^n$$

where, α is the absorption coefficient, $h\nu$ is the incident photon energy, A is constant and the value of n is 2 for a direct transition and $1/2$ for an indirect transition. In this case, $n = 2$ for the determination of optical direct band gap of Co_3O_4 nanoparticles. Insets of Fig. 3.3 shows the plots of $(\alpha h\nu)^2$ versus photon energy ($h\nu$). The band gap values of Co_3O_4 nanoparticles were calculated as 2.1 eV (590 nm), 2.5 eV (495 nm) and 3 eV (413 nm) using Tauc's relation for the samples calcinated at 200°C , 300°C and 400°C , respectively. This energy band gaps are greater

than those of bulk Co_3O_4 . The increase in the band gaps can be related to the quantum confinement effects of Co_3O_4 nanoparticles [13].

3.3.3. Photoluminescence study

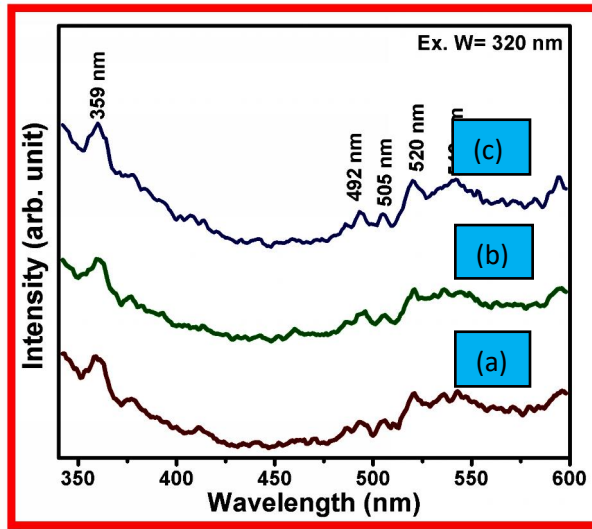


Fig. 3.4: PL emission spectra of Co_3O_4 nanoparticles calcinated at (a) 200° C, (b) 300° C and (c) 400° C

The photoluminescence emission spectrum can provide valuable information about the intrinsic and extrinsic defects in the crystals lattice of nanoparticles. Fig. 3.4. shows the room temperature PL emission spectra of Co_3O_4 nanoparticles calcinated at various temperatures. The samples were excited with an excitation wavelength of 320 nm. It is well known that the optical properties of Co_3O_4 nanoparticles are closely dependent on their structures and morphologies. In metal oxide nanostructures, the PL emission is usually classified into two sections including near band edge (NBE), UV emission and deep level (DL) defect associated to the visible emission. The UV emission is commonly attributed to the direct recombination of the excitons through an exciton-exciton scattering. The visible emission originates from the radiative recombination of a photo-generated hole caused by the impurities and structural defects in the crystal, for instance,

oxygen vacancies and cobalt interstitials. In general, the emission spectrum of the Co_3O_4 sample may have emission bands at 200-380 nm and 400-580nm wavelength ranges. The broad peak exhibited at 359 nm (3.5 eV) in UV region is due to the impact of calcination temperatures (200°C, 300°C and 400°C). The set of peaks observed at 492 nm (2.5 eV) and 520 nm (2.4 eV) were belongs to green emission. It is noted from the spectra that the intensity of UV emission is dominated than the visible emission, related that the surface morphology plays an important role for the determination of optical properties [14].

SUMMARY AND CONCLUSIONS

In the summary of present work, Co_3O_4 nanoparticles were successfully achieved by sol-gel method. The synthesized cobalt oxide nanoparticles were characterized by using XRD, UV-visible, PL studies. The XRD result confirmed the formation of simple cubic crystal structure of the Co_3O_4 . The average crystallite size of the samples are found to increase with increase in annealing temperature. The optical energy band gap values estimated by UV-visible analysis reported that the energy band gap values are increased with increase in calcination temperature. So that Co_3O_4 nanoparticles are used as p-type semiconductor. The Photoluminescence sharp peaks shows a near and edge emission located at UV region and green emissions. It is noted from the spectra that the intensity of UV emission is dominated than the visible emission related that the surface morphology plays an important role for the determination of optical properties. This method is simple, low cost, safe and suitable for the industrial production of high purity Co_3O_4 nanoparticles for various applications.

References

1. T. Pradeep, Nano: The essentials, ISBN-13:978-0-07-061788-9, (2009).
2. J. Kreuter, Int. J. Pharm., 331, pp:1-10, (2007).
3. Taylor and Francis, Handbook on Nanoscience, Engineering and Technology, 2nd edition.
4. Vollath D. Nanomaterials: an Introduction to synthesis, Properties and Application, Vol. 7, No: 6, pp: 865-870, (2008).
5. C.N.R. Rao, Annual Review of Physical Chemistry, Vol. 40, pp: 291-326, (1989).
6. Jia chen, Xifan wu, Annabella selloni, Phys. Rev. B 83, 24204, (June 2011).
7. Harish Kumar , Poonam Sangwan, Manisha, Advances in Applied Physical and Chemical Sciences-A Sustainable Approach - ISBN: 978-93-83083-72-5, pp: 99-103, (2017).
8. K.F. Wadekar, K.R. Nemade and S.A. Waghuley, Research Journal of Chemical Sciences, Vol. 7(1), pp: 53-55, January (2017).
9. Dr. S.V. Jagtap, A.S. Tale, S.D. Thakre, International Journal of Research in Engineering and Applied Sciences(IJREAS), ISSN (O): 2249-3905, Vol. 7, pp: 1~6, (August-2017).
10. M. Yarestani, A.D. Khalaji, A. Rohani, D. Das, Journal of Sciences, Islamic Republic of Iran 25(4), pp: 339-343, (2014).
11. Manish Shinde, Nilam Qureshi, Sunit Rane, Uttam Mulik, Dinesh Amalnerka, Physical Chemistry Communications, Vol. 2, Issue1, (May 2015).
12. Saeed Farhadi, Masoumeh Javanmard and Gholamali Nadri, Acta Chim. Slov., 63, pp: 335–343, (2016).

13. Saeed Farhadi, Jalil Safabakhsh and Parisa Zaringhadam, *Journal of Nanostructure in Chemistry*, 3:69, pp: 6-9, (2013).
14. G. Anandha Babu, G.Ravi, Y. Hayakawa, M. Kumaresavanji, *Journal Of Magnetism and Magnetic Materials*, 375, pp: 184-193, (2015)
15. S. K. Jesudoss, J. Judith Vijaya, P. Iyyappa Rajan, K. Kaviyarasu, M. Sivachidambaram, L.John Kennedy, Hamad A. Al-Lohedan and Jothiramalingam, *Photo Chemical and Photobiological Science*, March 2017 (Manuscript).
16. Guangmei Bai, Hongxing Dai, Jiguang Deng Yuxi Liu, Fang Wang, Zhenxuan Zhao, Wenge Qiu, Chak Tong Au, *Applied Catalysis A: General*, 450, pp: 42-49, (2013).

